Frequency dependence of tissue attenuation measured by acoustic microscopy

C. M. W. Daft
Department of Electrical and Computer Engineering, University of Illinois, 1406 W. Green Street, Urbana, Illinois 61801

G. A. D. Briggs
Department of Metallurgy and Science of Materials, Oxford University, Parks Road, Oxford OX1 3PH, United Kingdom

W. D. O'Brien, Jr.
Department of Electrical and Computer Engineering, University of Illinois, 1406 W. Green Street, Urbana, Illinois 61801

(Received 12 April 1988; accepted for publication 1 February 1989)

Broadband scanning acoustic microscopy (SAM) has been used to investigate the mechanical properties of sections of tissue with a resolution of around 8 μm. The work reported here extends these results by reporting the frequency dependence of the attenuation coefficient from 100–500 MHz. A discussion of the theory of the measurements is presented. The scanning laser acoustic microscope (SLAM) is used to characterize similar tissue sections at 100 MHz. The data obtained with the two forms of acoustic microscopy are compared with results from the literature.

PACS numbers: 43.80.Cs, 43.80.Ev, 43.35.Sx

INTRODUCTION

A method of acoustic time-domain reflectometry has been developed, which allows the elastic properties of a histological section to be measured with a resolution of around 8 μm.[1,2] This is accomplished by exciting the lens of an acoustic microscope with a voltage impulse from a step recovery diode. The impulse response of the lens used provided sufficient time resolution to separate the reflections from the top and bottom surfaces of a 10- to 15-μm section. This *A* scan can be analyzed to obtain the elastic properties of the interrogated point.

In this paper, the data from the experiment are processed so that the frequency dependence of the tissue attenuation is revealed. Comparisons are also made between SAM and SLAM data from similar tissue samples.

Leg muscle was used for this work. This tissue is striated and composed of cylindrical fibers that vary from 1–40 mm in length, and 10–100 μm in width. These fibers arise from the fusion of many myoblast cells and are multinucleate. Each fiber is surrounded by a fine network of collagen, the endomysium. The complete muscle is enclosed by a connective tissue layer, the epimysium, which holds the muscle together. This layer contains collagen fibers, which have great tensile strength, because of the way their principal amino acids (hydroxylysine and hydroxyproline) polymerize. Collagen has a static Young modulus 1000 times greater than most other types of tissue. In the epimysium, the fibers are interwoven into sheets. Individual fibers are 1–12 μm in diameter.

I. EXPERIMENTAL METHODS

The lower leg muscles of an adult ICR mouse were dissected and frozen in liquid nitrogen. Frozen 60-μm sections were cut transverse to the fiber direction using a Lipshaw cryostat for examination with the SLAM; adjacent frozen 14-μm sections were cut from the same block for investigation in the SAM. These sections were mounted unfixed on glass slides and imaged in pseudotransmission using a reflection microscope. Conventional images were made with a 60-ns tone burst and a receiver bandwidth of 10 MHz. The echoes from the specimen surfaces were completely mixed at this bandwidth.

When the lens is operated in impulse mode, an 11-ns pulse is received from a glass reflector (measured between its −20-dB points). A sampling oscilloscope was used to record the returning signal. After signal averaging and background subtraction, a signal-to-noise ratio of 51 dB at the center frequency (240 MHz) was achieved. The spectrum of the pulse is approximately Gaussian, but with a slower rate of decrease on the high-frequency side. The signal-to-noise ratio was 23 dB at 100 and 510 MHz; these frequencies were taken as the end points for measurements of the frequency dependence of attenuation.

Two pulses were generally recorded from tissue: the echoes from the tissue/water and tissue/glass interfaces. These were compared in the analysis with a reference signal, which was generated by moving the lens away from the tissue.

In Ref. 2, the reference signal (measured without tissue) is modeled in the frequency domain by the function

$$R(f) = M(f)\exp(2\pi j f t_3) \tag{1}$$

and

$$S(f) = AM(f)\exp(2\pi j f t_1) + \alpha(f)M(f)\exp(2\pi j f t_2) \tag{2}$$

for the signal with tissue. In these expressions, $M(f)$ is the

 0001-4966/89/052194-08$00.80

frequency response of the lens; A is a real constant; $\alpha(f)$ is a real function representing the frequency dependence of the tissue attenuation and the two-way transmission loss; and t_1, t_2, and t_3 are the time positions of the tissue/water, tissue/glass, and reference signals, respectively.

The two pulses are sufficiently widely spaced that the error involved in isolating the tissue/glass echo (by time gating) in order to compute its Fourier transform will be small. This transform was then deconvolved with the reference signal (1), and its magnitude was squared to produce a power spectrum. Frequency-domain data are also needed to Wiener filter the data. The function

$$w(t) = \mathrm{FFT}^{-1}\left(\frac{S(f)R^*(f)}{R(f)R^*(f) + N^2}\right) \tag{3}$$

(where N^2 is a constant that depends on the noise level) gives an approximation to the impulse response of the tissue.

The thickness of the section is computed by forming the cross correlation of the first pulse and the reference signal, and finding its maximum. Homomorphic deconvolution is used to calculate the separation of the two pulses, which determines the velocity. Changes in the acoustic impedance of the tissue cause fluctuations in the size of the tissue/water pulse. The cross-correlation function's maximum value is normalized by the reference signal to obtain the reflectance at the tissue surface. Attenuation data are obtained by comparison of the tissue/glass pulse, which has passed through the section twice, with the reference signal.

In this experiment, the errors in velocity and thickness due to temperature variations in the coupling fluid, and deviations from a perfectly flat lens scan, are 5%. These appear to dominate the systematic error caused by assumptions in the model of the experiment.[2] The impedance error is largely systematic, varying from 1% at $Z = 1.6$ Mrayl to 10% at $Z = 2.05$ Mrayl. The accuracy of the attenuation measurements is assessed in Sec. III.

II. RESULTS

Figure 1(a) shows a tone burst scanning acoustic microscope image obtained with the lens (500-μm focal length, $F/1$) focused on the surface of the microscope slide, at a frequency of 425 MHz and a field of view of 425 μm. The beamwidth is 5 μm at the focus, using the Rayleigh criterion. Fibers of both the soleus and gastrocnemius muscles are visible, as is the epimysium. "Time-resolved line traces" are B scans (in contrast to the C scan of a tone burst SAM image) but differ from the clinical and NDT types by the omission of demodulation or time gain control. Figure 1(b) is such a time-resolved line trace, taken just to the left of the dashed

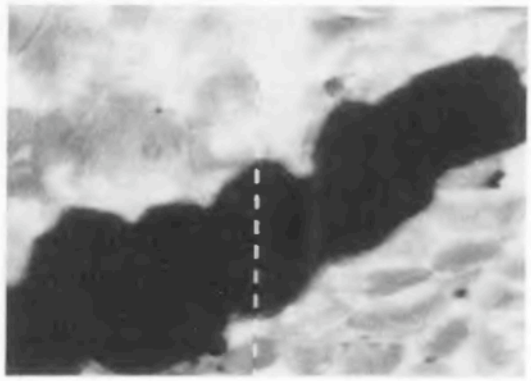

(a) SAM image (425 μm fov)

(b) Time resolved linescan (600 μm fov)

(c) Optical image (2.8 mm fov)

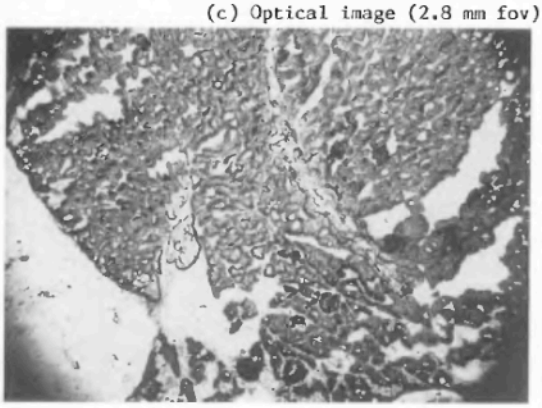

(d) Wiener filtered linescan (600 μm fov)

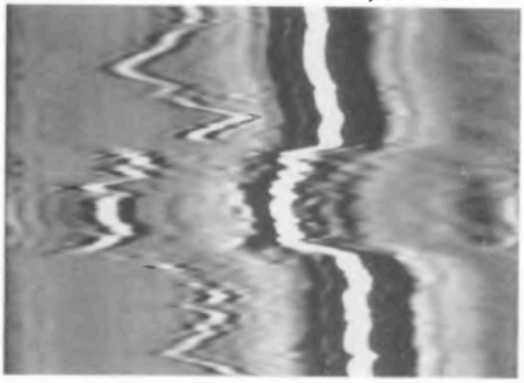

FIG. 1. Images of a transverse section of mouse leg showing soleus and gastrocnemius muscles, and the margin between them (epimysium). The tone-burst image (a) has a 425-μm field of view (fov) in which the epimysium appears very dark; (b) is a time-resolved linescan taken along a path corresponding to the dashed line in (a); (c) is an optical image of an adjacent section; (d) shows a Wiener filtered version of (b). The horizontal axis is time, with a 50-ns field of view. Pixel brightness is determined by the voltage received by the sampling oscilloscope.

line in Fig. 1(a). The scan begins at the top of Fig. 1(a), but is 600 μm long. The dashed line in Fig. 1(a) thus indicates the top 71% of the line trace of Fig. 1(b). The horizontal axis of this image is time, with a total scan of 50 ns. The vertical axis corresponds to the position of the lens. Picture brightness is proportional to detected voltage, so the no-signal level is grey and received signals appear as a succession of black and white stripes. Two pulses are generally visible; a tissue/glass echo to the right, and a weaker tissue/water echo on the left. The black region of the SAM image in Fig. 1(a) is connective tissue between the two muscles; it causes a large shift to the left in the second pulse on the time-resolved linescan. This connective tissue is visible at lower magnification in Fig. 1(c), which is an optical micrograph of the adjacent frozen section cut. The tissue section is stained with toluidene blue and has a field of view of 2.8 mm. The effect of applying a Wiener filter to the data is shown in Fig. 1(d).

The time-resolved data were analyzed by the method described in Ref. 2; results are plotted in Fig. 2 from the top of Fig. 1(a) to the lower boundary of the collagen. Large variations were observed in the sample thickness; a nominally 14-μm section varies from 6.2 to 17.5 μm. The velocity figures show typical tissue values of 1550–1600 m s^{-1} for the muscle fibers, while the connective tissue has a peak of slightly over 2000 m s^{-1}. The impedance is also considerably larger in the connective tissue. The mean value of the frequency-averaged attenuation coefficient is 86 dB mm^{-1}, which may be compared with the figure of 45 dB mm^{-1} obtained in kidney tissue at 222 MHz.[3] However, the peak value of the attenuation coefficient in the epimysium is much higher, at 400 dB mm^{-1}, reflecting the anomalous behavior of the structural protein collagen.

For comparison purposes, a 60-μm slice of tissue (adjacent to the section used above) was investigated in a SLAM at 100 MHz. The SLAM is a transmission technique,[4] in which attenuation is the primary source of contrast in the intensity image. The interference image is mainly dependent on the velocity distribution in the sample. Figure 3 shows the results; in each case, the field of view is 3 mm horizontally by 2 mm vertically. Figure 3 (a) is an optical image of the sample; the connective tissue is visible as the darker band in the center of the image. Figure 3(b) is the acoustic amplitude image; it can again be seen that the attenuation is higher in the muscle boundary than the surrounding tissue. Figure 3(c) is the interference image. The sample is surrounded by saline, which is used as a reference medium, in which the fringes are spaced at 85-μm intervals. A shift of the fringes to the right, which can be observed at the boundaries of the specimen, indicates an increase in velocity. The high attenuation in the muscle boundary near the bottom of the image conceals a further increase in velocity there. The graph of Fig. 3(d) shows the velocity variation through a vertical line down the center of the images; these values were computed by the method described in.[4]

The saline reference at the top has a velocity of 1520 m s^{-1}, while the connective tissue velocity peaks around

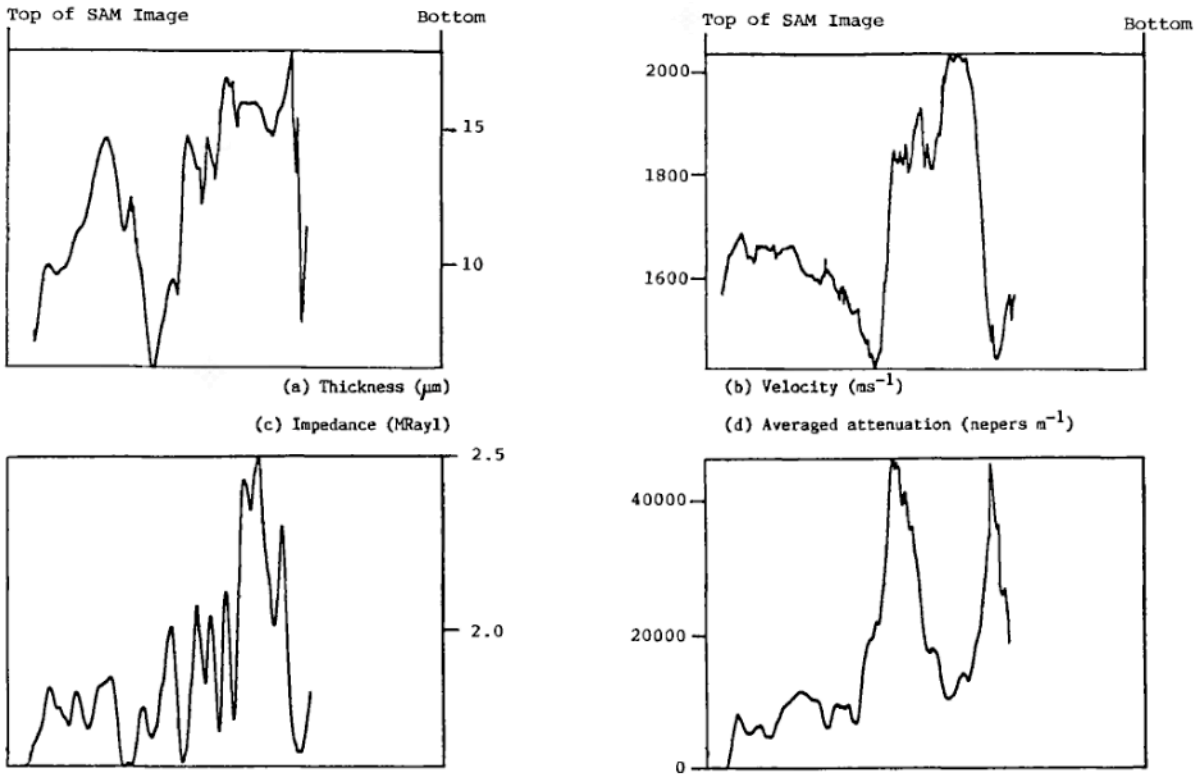

FIG. 2. Elastic properties of the section as computed from the data of Fig. 1(b). The left-hand side of each of the graphs corresponds to the top of Fig. 1(b). Notice the high velocity and attenuation in the connective tissue [center of (b) and (d)].

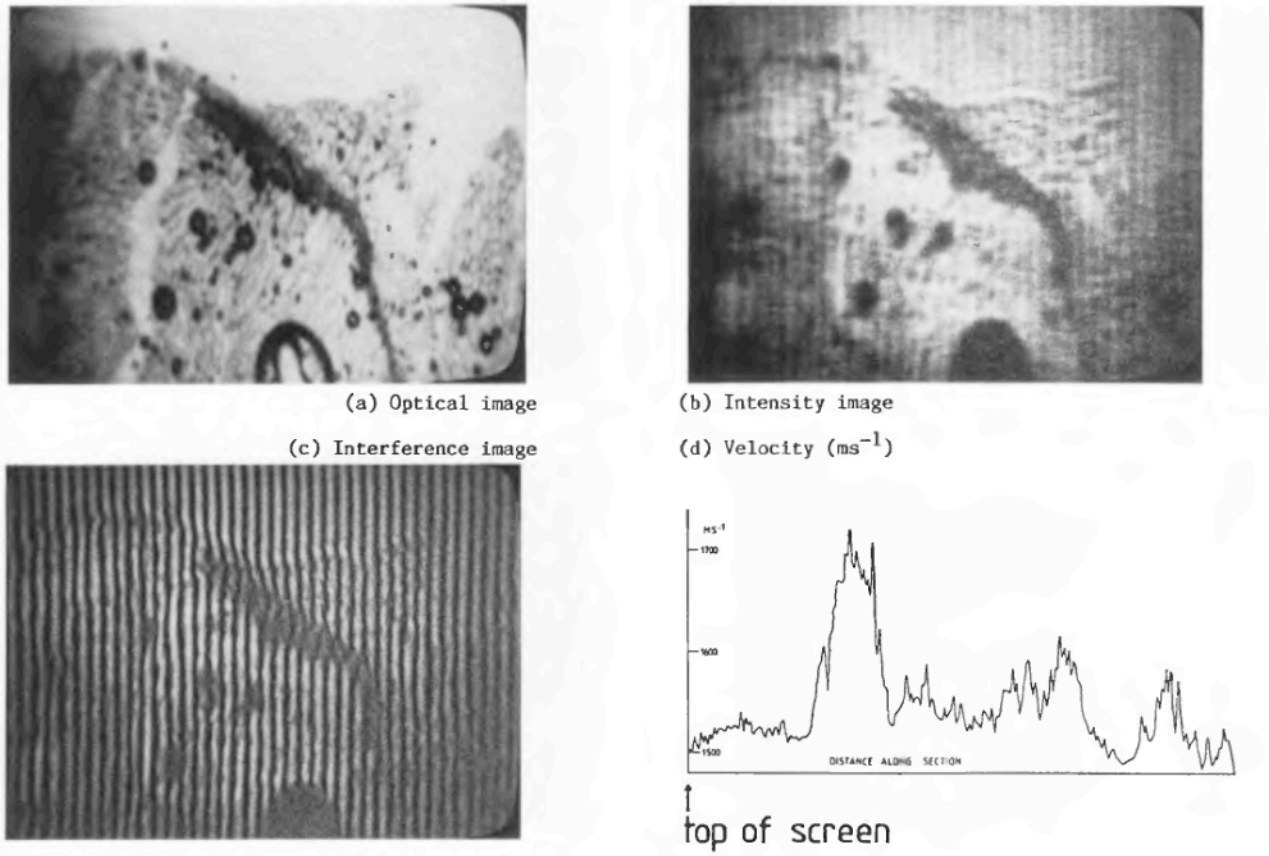

FIG. 3. Results obtained with the SLAM on an adjacent section (nominal thickness = 60 μm; acoustic frequency = 100 MHz; field of view = 3 mm × 2 mm); (a) shows the optical image; (b) and (c) are acoustic. The muscle boundary appears dark in the intensity image (b) due to its high attenuation. A graph of velocity (d) computed for the vertical bisector of the interferogram (c) indicates enhanced velocity in this boundary.

1720 m s^{-1}. This increased velocity correlates with that observed in the SAM; however, the measured maximum velocity is 15% less in the SLAM. The measurement in the SLAM is of a phase change, so that the tissue thickness is needed to calculate the velocity. As can be seen from the range of thicknesses in a nominally 14-μm section, this parameter cannot be controlled accurately. Furthermore, the resolution cell is considerably larger in the SLAM than in the SAM, which might be expected to moderate large local variations in acoustic parameters. It also proved impossible to avoid dehydration of the SAM sections in the journey between our laboratories, which has been shown to increase tissue velocities.[5]

The fact that the time-resolution experiment can provide values for the attenuation over more than 2 octaves of hitherto unexplored spectrum is perhaps its major advantage. The rest of this paper will present some results computed from the present specimen, and another section. This will be followed by a discussion of the validity of the data.

As described in Sec. I, the tissue/glass pulse, which has passed through the tissue twice, can be analyzed to yield the frequency dependence of the tissue attenuation. The signal was deconvolved with the reference signal and a power spectrum was calculated. Figure 4(a) displays the results pictorially.

The left-hand side of the image represents a frequency of 100 MHz, and the right-hand side is 510 MHz. The vertical axis is the same as in Fig. 1(b); it represents distance along the sample (600 μm). Pixel brightness represents the intensity of the deconvolved signal at a given frequency and position. This presentation allows the spatial variations of the spectral response of the tissue to be examined. In order to allow a quantitative assessment of this image, it has been segmented into five grey levels. Areas of white correspond to deconvolved intensities of between 0.7 and 1.0. The next three grey levels are contoured at 0.5, 0.3, and 0.1, and black indicates a signal of lower intensity than 0.1. The area at the top of the image (which is an area where there is no tissue) is uniformly white. In the muscle tissue, a general decrease of signal with increasing frequency is observed. Figure 5(a) shows a typical muscle spectrum, where the attenuation is roughly proportional to frequency. When a similar spectrum was calculated from data from a fat cell, the attenuation[6] was found to vary as $f^{1.66}$. This is the same as the accepted value for castor oil.[7] In stark contrast to this, very little signal is observed at low frequencies from the collagen in the middle of the picture. Instead, the signal rises to a maximum at around 240 MHz, and then decreases sharply [Fig. 5(b)]. This behavior was observed throughout the middle of the connective tissue area, but not at its edges. Figure 5(c)

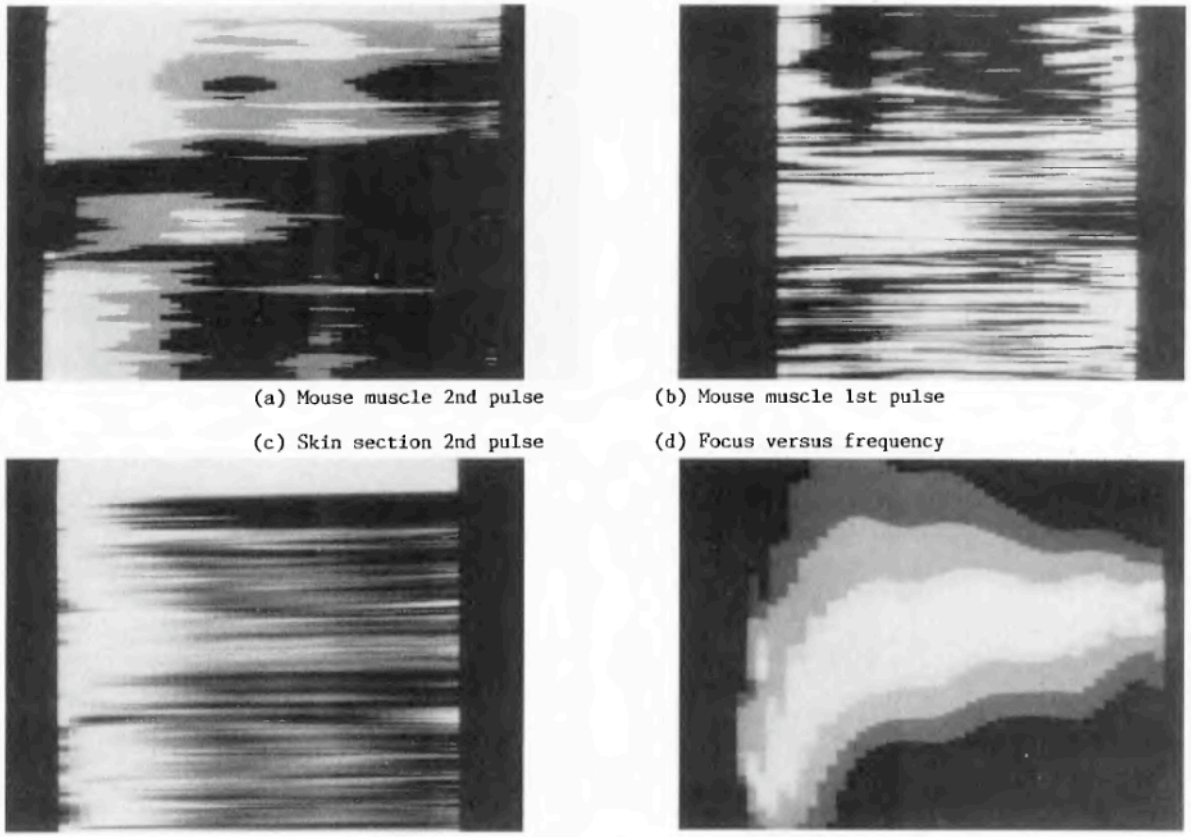

FIG. 4. Deconvolved power spectra obtained with the broadband acoustic microscope, displayed with image brightness proportional to received power. The vertical axis is distance; the field of view is 600 μm in (a) and (b) (as in Fig. 3); (c) has a field of view of 705 μm. The horizontal scale is frequency: 100 to 510 MHz in (a), (c), and (d), and 120 to 480 MHz in (b). The anomalous behavior of the epimysium can be seen in the central part of (a); this corresponds to the area of high velocity and attenuation in Fig. 1(b). (d) indicates the movement of the focal point of the lens with frequency; the vertical scale covers 28 μm of defocus.

shows the behavior of the edge, which exhibits peaks in its spectrum at 160 and 280 MHz.

A peak in the received signal implies that constructive interference from the sides of a structure in the tissue is occurring. Since the sound velocity in this area is 1900–2000 m s^{-1}, the wavelength of sound at 240 MHz is 8 μm. A tentative hypothesis to explain this effect would be that there are one of more $\lambda/2 = 4$-μm collagen fibers inside the section at this point. The deconvolved spectrum of the first pulse was also computed, and the result is shown in Fig. 4(b). Because there is such a large variation in the size of the first pulse, each line has been normalized. The contours are at 0.8, 0.5, 0.3, and 0.1 of the maximum value in that line. Data are only presented in the range 120–480 MHz because of signal-to-noise constraints. However, the reflection from the collagen is very strong, and a peak in the spectrum at 240 MHz is again observed, confirming the "resonance" in the second pulse. The peak at this frequency is not a feature of collagenous tissue, in general; other muscle boundaries were investigated in the same way, and different behavior was found, e.g., that in Fig. 5(d). From 120–350 MHz, this sample shows an increase in signal strength with frequency. There is also a gentle dip in the signal around 430 MHz, and even a suggestion that a peak may occur above that frequency. These frequencies would also predict a characteristic dimension in the correct range for collagen fibers (1–12 μm).

It must be emphasized that more work is needed to interpret these spectra. A spectrum from a section of skin is shown without contouring, but with each line normalized, in Fig. 4(c). Again, there is no tissue at the top of the linescan, so the data appear uniformly bright there. One can only conclude from this image that the tissue attenuation generally increases with frequency. At this microscopic scale, there is considerable variation in the rate at which attenuation increases throughout the section, so the image appears striated.

III. DISCUSSION

A separate question is the reliability of the frequency spectrum data. The signal-to-noise ratio of the tissue/glass pulse is sufficiently good that the major source of experimental error in the time-resolved traces is due to drift in the sampling oscilloscope amplifiers ($\pm$ 3%). Water temperature and scan flatness are not so important as in the measurement of tissue thickness and velocity. However, several possible sources of systematic error need to be considered. As has been noted, the lens was focused halfway down the sec-

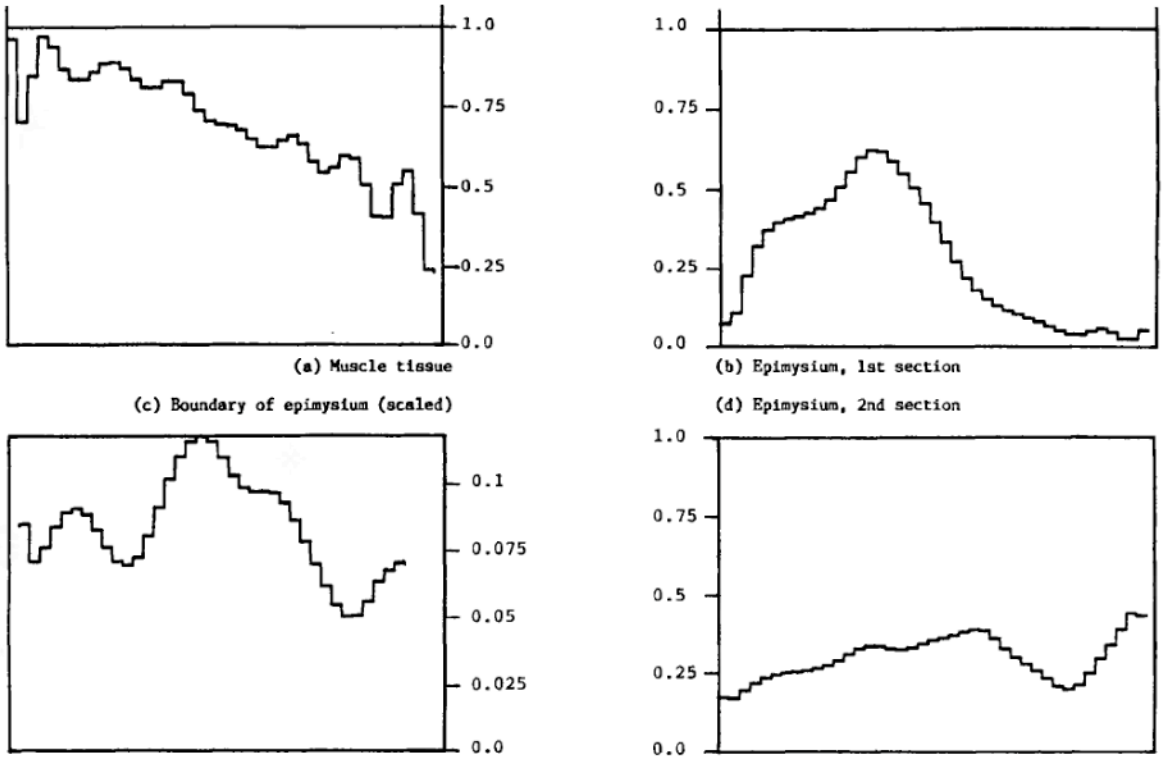

FIG. 5. Deconvolved power spectra of the second pulse plotted from 100 to 510 MHz. Attentuation roughly proportional to frequency is observed in (a). The widely differing behavior of the epimysium (b), (c), and (d) suggests an inhomogeneous acoustic structure on this scale.

tion at 250 MHz. The position of this focus will change with frequency, and it seemed possible that the convergence of the lens might corrupt the data in some frequency-dependent way.

In order to investigate this, the variation of the position of the lens focus with frequency was measured. The most convenient way to do this was using a glass slide reflector and the time-resolution apparatus. The lens output was recorded for a 28-μm vertical sweep, which included the focus. Each time trace was Fourier transformed and a power spectrum was computed. No deconvolution was performed, but each $V(z)$ was normalized to eliminate the variation of transducer efficiency with frequency. The result of this experiment is shown in Fig. 4(d). In this image, the horizontal axis again represents frequency, from 100–510 MHz. The vertical axis is z, the vertical position of the lens. The image is contoured; ultimate white represents a normalized power of greater than 0.95, and the other transitions are at 0.9, 0.7, and 0.5. Under 0.5 appears as black. As the frequency is increased, the focus becomes tighter, as might be expected. At 250 MHz, a 10% variation in acoustic power occurs over a vertical distance of 8.5 μm. It is interesting to note the lack of movement of the focal position from 200 to 510 MHz. Below 200 MHz, diffraction effects are causing the focus to move somewhat more.

The effect of this on the time-resolution data can be understood with reference to Fig. 6. In this diagram, the tissue/water interface has z coordinate z_1 and the surface of the glass slide is at z_2. Both of these distances are measured from $z=0$, defined as the focus of the lens at its center frequency f_c. The locus of the maxima in Fig. 4 (d) is denoted by $b(f)$, which is positive for $f>f_c$, and negative for $f<f_c$.

If the focusing action of the lens is now taken into account, the output of the lens with tissue at a frequency f is obtained by modifying (2),

$$S'(f) = M(f)[A\exp(2\pi jft_1)V_G(z_1,f) + \alpha(f)\exp(2\pi jft_2)V_G(z_2,f)], \quad (4)$$

where $V_G(z,f)$ is the lens output at a defocus z and frequency f, without tissue, i.e., the data of Fig. 4(d). The reference signal can be written as

$$R'(f) = M(f)\exp(2\pi jft_3)V_G(z_2,f), \quad (5)$$

neglecting water attenuation in the thickness of the section. The assumption about V_G implicit in the expressions (1) and (2) for $R(f)$ and $S(f)$ can now be quantified as

$$V_G(z_1,f) \simeq V_G(z_2,f) \quad (6)$$

for all f of interest. Inspection of Fig. 4(d) shows this to be a reasonable assumption for frequencies above 200 MHz.

The effect on the power spectra measurement can be calculated by dividing the first and second terms in (4) by the reference signal, and taking the squared magnitude. The first pulse spectrum is scaled by

$$|V_G(z_1,f)/V_G(z_2,f)|^2,$$

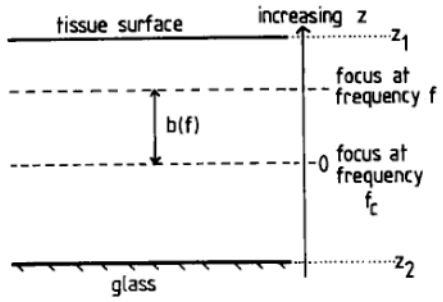

FIG. 6. Geometry used for calculating the effect of focal length variations with frequency.

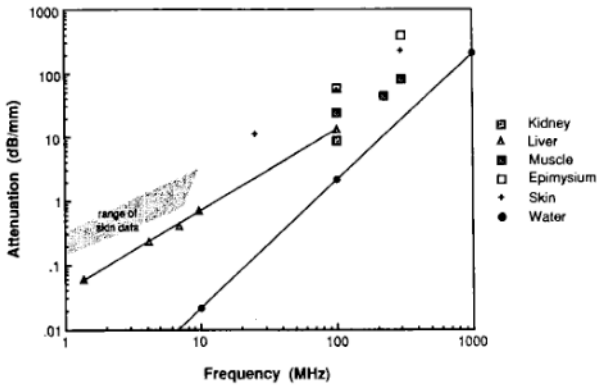

FIG. 7. SAM and SLAM results compared with data from the literature. For reference, the attenuation of water and typical parenchyma (liver) are included. The box indicates the range of skin data from Refs. 8–11. Note that the highest attenuation value obtained is not comparable to the other points on the graph (see text).

but the focal length effect cancels in the power spectrum of the second pulse: It is still $\alpha^2(f)$. Therefore, the deconvolution results are accurate regardless of whether V_G conforms to Eq. (6).

There are still two approximations in this analysis. Identifying $(10/x)\log_{10}\alpha^2(f)$ with the tissue attenuation in dB, where x is the section thickness, assumes that only a small amount of the incident power is reflected at the tissue/water interface. This is a good approximation for most tissue, where the first echo is 20–30 dB smaller than the reference signal. In the collagen, the power spectrum of the second pulse will be reduced by about 10% at the frequency at which there is a maximum in the first pulse spectrum. This means that the 240-MHz peak in Fig. 4(b) is, in fact, larger than the graph shows.

Second, no allowance has been made for changes in focal length with tissue velocity. This will affect the measurement of the spectrum of both pulses. A rough calculation for the lens used gives around 3 μm of movement with 2000-ms^{-1} tissue (the worst case). From Fig. 4(d), it can be seen that this would have the most effect at 500 MHz. At this frequency, the acoustic power in the second pulse will be underestimated by some 10%, since the focus moves in the positive z direction. This could be corrected by multiplying the power spectrum by a filter. The response of this filter could be computed from the tissue velocity and the data of Fig. 4(d).

Another concern is the possibility that variations in tissue thickness on a scale smaller than the resolution cell will cause phase cancellation. This would lead to inflated attenuation estimates. However, it is hard to reconcile the gradual changes in acoustic properties [e.g., in Fig. 4(a)] with significant phase cancellation, which would produce alterations in the spectra of adjacent pixels.

IV. COMPARISONS WITH PUBLISHED DATA

Figure 7 shows selected results on the frequency dependence of attenuation for five types of tissue. The box shows the range of data on skin from 1–10 MHz, as given in Refs. 8–11. Data from the SAM have been averaged over the 100- to 500-MHz range, and are recorded at 300 MHz. The skin data from the SAM measurements were obtained by averaging the received signal through the dermis of a guinea pig.[2] At 100 MHz, the result is a mean value from 60 measurements on canine skin,[12] while the 25-MHz result from the same publication was obtained from a backscattering technique.[13] The two points recorded for epimysium are not directly comparable; the 100-MHz (SLAM) measurement is a mean value for the complete muscle boundary, averaged over several specimens. As can be seen from Fig. 2, this tissue appears very inhomogeneous in the higher resolution SAM results. The peak value is therefore recorded at 300 MHz on the graph. The images of the muscle fibers revealed milder variations in attenuation, and were also plotted at 100 and 300 MHz. For reference, the attenuation of water and liver[14] are included. Liver is an example of typical parenchyma, with a relatively low attenuation that is proportional to $f^{1.27}$, whereas the value for water is proportional to f^2.

It seems reasonable to suppose that tissue must always attenuate sound more than water; thus, at some frequency, the slope of the line drawn through the liver data must increase. Kessler[3] observed such a change in mammalian kidney (his data are shown on the graph), which contrasted with the linear dependence at lower frequencies.[15] In the present work, the behavior of both skin and muscle appears similar in the 100- to 300-MHz range to the 1- to 100-MHz liver data. The intercept of the lines with the attenuation axis varies (skin attenuates more because of the higher structural protein content), but the slope does not approach the f^2 exhibited by water.

V. CONCLUSIONS

The impulse-excited SAM has been used to measure the frequency dependence of attenuation in muscle fibers, connective tissue, and skin. This method is simple to implement and capable of producing accurate results. Comparisons with other techniques can be made if the SAM data from a similarly sized area of tissue are averaged. This eliminates the fine structure [e.g., in Fig. 4(c)] caused by microscopic variations. The muscle fibers and skin tissue appear to have the same frequency dependence of attenuation in the SAM range as at lower frequencies. This allows a conclusion to be drawn about the dispersion from 100- to 500-MHz. As O'Donnell *et al.* have shown,[16] a linear increase in attenuation causes less than 0.2% velocity change from 1 to 10

MHz. Since the approximate $f^{1.3}$ dependence seems to hold for skin and muscle fibers, a large dispersion over the 100- to 500-MHz range is not expected.

Tissue with a high concentration of structural protein has anomalous behavior. This may be due to the fibers being of comparable size to the acoustic wavelength. Further work is needed to evaluate the peaks that were characteristic of the power spectra of some of the received signals. This behavior also will have interesting consequences for the dispersion.

ACKNOWLEDGMENTS

We would like to thank the following for their contributions to this work: Dr. J. M. R. Weaver, Dr. M. G. Somekh, Dr. J. M. Rowe, Dr. I. R. Young, Dr. D. M. Shotton, and Dr. J. Carnwath. Particular thanks to Dr. J. Kushibiki of Tohoku University, Sendai, Japan, whose excellent acoustic lens made this work, and that reported in Refs. 1, 2, and 6, possible. Financial support for this project was furnished by SERC, GEC Hirst Research Center and the National Institutes of Health (CA36029).

[1]C. M. W. Daft, J. M. R. Weaver, and G. A. D. Briggs, "Tissue characterization with microscopic resolution," Proc. 1986 IEEE Ultrasonics Symposium (IEEE Publ. No. 86CH2375-4).

[2]C. M. W. Daft and G. A. D. Briggs, "Wideband acoustic microscopy of tissue," IEEE Trans. Ultrason. Ferroelectr. Freq. Control **UFFC-36**(2) (1989).

[3]L. W. Kessler, "VHF ultrasonic attenuation in mammalian tissue," J. Acoust. Soc. Am. **53**, 1759–1760 (1973).

[4]P. M. Embree, K. M. U. Tervola, S. G. Foster, and W. D. O'Brien, Jr., "Spatial distribution of the speed of sound in biological materials with the scanning laser acoustic microscope," IEEE Trans. Sonics Ultrason. **SU-32**, 341–350 (1985).

[5]S. A. Goss and W. D. O'Brien, Jr., "Direct ultrasonic velocity measurements of mammalian collagen threads," J. Acoust. Soc. Am. **65**, 507–511 (1979).

[6]C. M. W. Daft and G. A. D. Briggs, "The elastic microstructure of various tissues," J. Acoust. Soc. Am. **85**, 416–422 (1989).

[7]F. Dunn, P. D. Edmonds, and W. J. Fry, "Absorption and dispersion of ultrasound in biological media," in *Biological Engineering*, edited by H. P. Schwan (McGraw-Hill, New York, 1969), pp. 205–332.

[8]P. K. Bhagat and W. Kerrick, "Ultrasonic characterization of aging in skin tissue," Ultrasound Med. Biol. **6**, 369–375 (1980).

[9]M. Oka, "Progress in studies of the potential use of medical ultrasound," Wakayama Med. Rep. **20**, 1–50 (1977).

[10]N. Nakaima *et al.*, "Supplementary study of the ultrasonic absorption of human soft tissue," J. Wakayama Med. Soc. **27**, 107–115 (1976) (in Japanese).

[11]K. T. Dussik *et al.*, "Measurements of articular tissues with ultrasound," Am. J. Phys. Med. **37**, 160–165 (1958).

[12]M. A. Riederer-Henderson, J. E. Olerud, W. D. O'Brien, Jr., F. K. Forster, D. L. Steiger, D. J. Ketterer, and G. F. Odland, "Biochemical and acoustical parameters of normal canine skin," IEEE Trans. Biomed. Eng. **35**, 967–972 (1988).

[13]F. K. Forster *et al.*, "Ultrasonic assessment of skin and surgical wounds utilizing backscatter acoustic techniques to estimate attenuation," Ultrasound Med. Biol. (in press).

[14]J. D. Pohlhammer, C. A. Edwards, and W. D. O'Brien, Jr., "Phase insensitive ultrasonic attenuation coefficient determination of fresh bovine liver over an extended frequency range," Med. Phys. **8**, 692–694 (1981).

[15]S. A. Goss, R. L. Johnston, and F. Dunn, "Comprehensive compilation of empirical ultrasonic properties of mammalian tissues," J. Acoust. Soc. Am. **64**, 423–457 (1978).

[16]M. O'Donnell, E. T. Jaynes, and J. G. Miller, "Kramers–Kronig relationship between ultrasonic attenuation and phase velocity," J. Acoust. Soc. Am. **69**, 696–701 (1981).